A Physical Model for Dynamical Arthropod Running on Level Ground

Haldun Komsuoğlu§ Kiwon Sohn§ Robert J. Full† Daniel E. Koditschek§

haldunk@seas.upenn.edu kiwon@seas.upenn.edu rjfull@socrates. berkeley.edu kod@seas.upenn.edu

§Department of Electrical and Systems Engineering, University of Pennsylvania, PA, USA
†Department of Integrative Biology, University of California, Berkeley, CA, USA

May 30, 2008

Abstract

Arthropods with their extraordinary locomotive capabilities have inspired roboticists, giving rise to major accomplishments in robotics research over the past decade. Most notably bio-inspired hexapod robots using only task level open-loop controllers [22, 9] exhibit stable dynamic locomotion over highly broken and unstable terrain. We present experimental data on the dynamics of *SprawlHex* — a hexapod robot with adjustable body sprawl — consisting of time trajectory of full body configuration and single leg ground reaction forces. The dynamics of *SprawlHex* is compared and contrasted to that of insects. *SprawlHex* dynamics has qualitative similarities to that of insects in both sagittal and horizontal plane. *SprawlHex* presents a step towards construction of an effective physical model to study arthropod locomotion.

1 Introduction

Rapidly running insects demonstrate high maneuverability [28] and can recover by mechanically induced restoring forces whose time constants are too fast to be associated with neural reflex loops [7] from very large lateral perturbations as well [18].

It is now generally recognized that the passive mechanical properties of a robotic platform not only facilitates handling complex obstacles [26] but also play a pivotal role in production of stable dynamic behaviors [12, 20, 13, 18]. Insect runners produce sizable non-propulsive lateral forces [28], believed to play an important role in behavioral stabilization [11]. Characterization of the mechanisms responsible for insects' enviable horizontal plane agility can greatly benefit robotic designs, could we understand how they function and how to harness them.

Simple, single-legged sagittal-plane [16, 15] and horizontal-plane [23, 24], template [14], models of dynamical locomotion have been shown mathematically to exhibit aspects of mechanical self-stabilization first hypothesized in numerical studies [20]. However, teasing out the neural ("reflex") from purely mechanical ("preflex") mechanisms of stabilization has proven to be very challenging, both mathematically [4, 3], as well as biologically [2]. Our long term goal in this study is to bring the light of physical empiricism to bear on this important but complicated set of questions and design opportunities. In this paper we test the hypothesis that a mere change in body posture from an upright to laterally sprawled hip attachment orientation can induce insect-like horizontal plane force patterns with no alteration of the control strategy. In subsequent studies we will explore the consequent implications for locomotory stability.

The paper is organized as follows. Section 2 introduces *SprawlHex* — a programmable hexapod robotic platform with manually adjustable body sprawl. Section 3 describes our experimental setup which provides us syn-

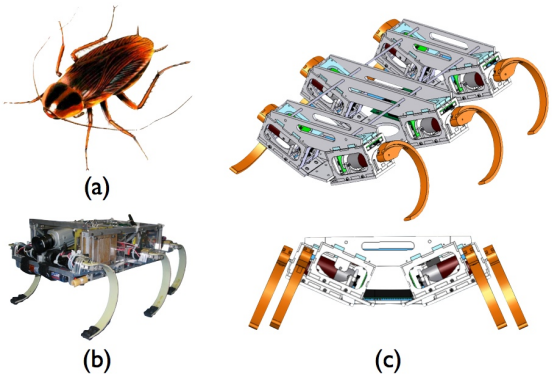

Figure 1: (a) A representative target biological system, the cockroach. (b) the predecessor bio-inspired highly mobile robotic platform, the RHex robot [22] (c) *SprawlHex* CAD model from two perspectives. The frontal view in the bottom demonstrates the manually adjustable sprawl posture.

chronized high resolution (temporal and spatial) measurements of single leg ground reaction forces, full body pose, and proprioceptive sensory data. The data collection conventions are defined in Section 4. Section 5 presents various preliminary analysis of the collected data, comparing and contrasting the dynamic characteristics of arthropod locomotion to that of *SprawlHex* . Statistical analysis of single leg ground reaction forces (GRF) in Section 5.1 relate the sprawl posture and the magnitude of the lateral ground reaction forces. Section 5.2 focuses on the dynamic roles of leg pairs. A system identification and verification analysis is outlined in Section 7. The discussion follows in Section 8.

2 *SprawlHex* Platform

The *SprawlHex* robot in Figure 2 is a computationally autonomous and battery powered hexapod platform. The fully loaded robot weighs 3 kg and measures 40 (L) x 30 (W) x 8 (H) cm. *SprawlHex* construction is founded on a modular and extensible electromechanical toolkit [19] which has been successfully employed in various research and education robots [29, 10, 17]. The computational infrastructure of the system consist of a Pentium class CPU running Linux OS and a suite of embedded controllers. The peripheral embedded devices are linked to the central processor by a custom communicational infrastructure, RiSEBus, which was originally developed for the RiSE robot [6]. Hard real-time control processes are performed by distributed embedded controllers that receive low frequency parsimonious commands from soft real-time high level behavioral controllers running on the central CPU.

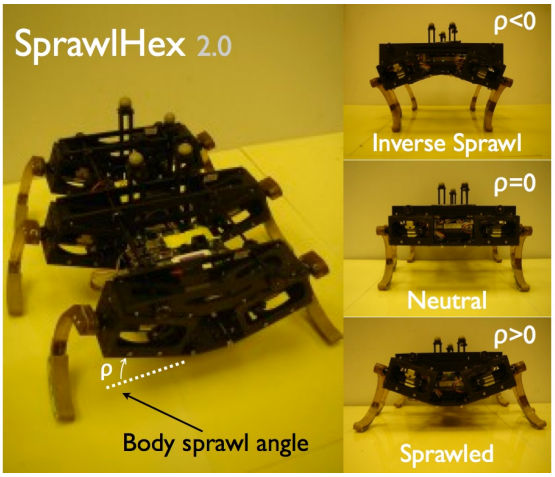

Figure 2: *SprawlHex* adopts a the hexapod RHex morphology and permit manual configuration of the leg sprawl where the leg sprawl, ρ, (or body sprawl) is the angle between the axis of the hip rotor and the horizontal body plane. On the right hand side three classes of sprawl configurations are demonstrated: inverse sprawl, $\rho < 0$; neutral, $\rho = 0$; and sprawled, $\rho > 0$.

SprawlHex adopts a variant of the hexapod morphology which was first introduced by the RHex robot [22] and was also employed in a smaller and cheaper implementation, EduBot [29]. Its six legs are symmetrically arranged in groups of three on two sides of the body supporting its rigid body which encapsulates all actuators, electronic infrastructure and batteries.

The design of SprawlHex differs from its predecessors RHex in that its body sprawl is manually adjustable. Although it seems to be a small modification, this configurable passive mechanical property of the robot is the

corner stone of this study. In the RHex platform lateral ground reaction forces (GRF) are the product of the passive lateral compliance of legs and cannot be actively excited. In contrast sprawled posture of *SprawlHex* partially aligns the active actuation with the lateral direction resulting in a limited but yet significant affordance on the lateral GRF production. Figure 2 demonstrates three class of sprawl configurations: inverse sprawl, $\rho < 0$; neutral, $\rho = 0$; and sprawled, $\rho > 0$.

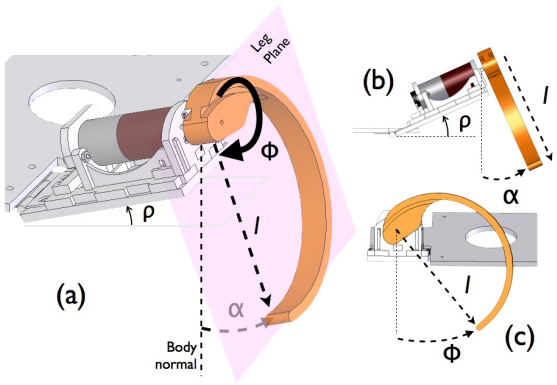

Figure 3: Kinematic configuration of *SprawlHex* legs. The *sprawl angle* defined as the angle between the axis of the hip motor and the horizontal body plane, ρ. This term is also called the body sprawl. For ease of discussion we treat each leg as a compliant prismatic joint (from hip to toe) that is attached to the body at a universal joint (the wing and hip rotational DOF). The three dof configuration of each leg is represented by the wing angle, α, hip angle, ϕ, and the leg length, l. Notice that the wing configuration, α, and the body sprawl, ρ, are identical in the rest configuration but will differ under load since the leg is compliant.

Figure 3 defines various kinematic configuration details for a single leg. We treat each leg as a prismatic passive compliant appendage that is attached to the body at a universal joint. The leg length, l, the distance from hip attachment to the toe, and the leg wing angle, α, the angle between leg plane and the body normal, are passive degrees of freedom that are actuated by the compliance of the leg. Each leg has a single actively actuated degree of freedom that drives the hip angular position, ϕ. The rest posture of the wing angle, α, defines the body sprawl, ρ.

Figure 4: Half circle padded leg. (a) Half circle leg supporting the body, and (b) a close up of the leg showing the shape memory foam padding and rubber coating.

The legs (see Figure 4) are 12 cm diameter half circle passive compliant parts manufactured using the Shape Deposition Manufacturing (SDM) method [8]. This prototyping process permits us to simultaneously control various mechanical properties such as compliance and damping and their variation across the leg structure. The outside face of the leg is padded with shape memory foam and covered with 2 mm thick rubber. The foam padding offers damping to smooth out impacts with the ground. Up on ground contact the foam conforms to establish a good contact with the terrain independent of the sprawl angle. The rubber cover provides improved traction.

3 Experimental Setup

We constructed an experimental setup to facilitate systematic data collection in carefully controlled environmental conditions. Figure 5(a) depicts a typical experiment setup. Experiments are conducted on a 5 m long and 1.5 m wide runway. The surface of the runway is layered with a high friction surface (industrial carpet and/or sand paper) to

minimize slippage. The full body posture of the robot is captured by a high-end Vicon motion capture system (Figure 5(b)). A 6-DOF force plate (Figure 5(c)) embedded in the runway provides us with ground reaction force measurements from individual legs. The software on SprawlHex (Figure 5(d)) performs the behavioral control and collects proprioceptive sensory information such as instantaneous leg configurations and hip output torque. An external high speed video camera running at 120Hz is positioned to record each run in the horizontal and sagittal plane. The authors employ the video recordings to identify the force plate contacts and potential failures in experiments.

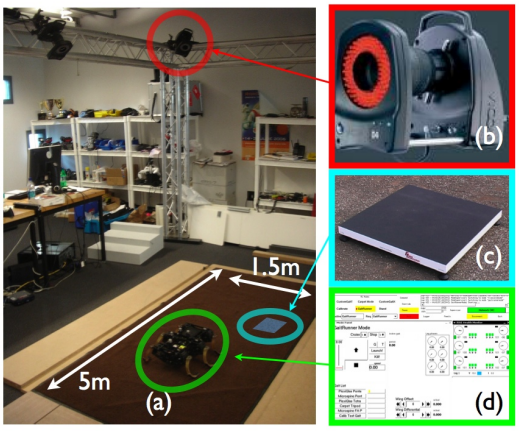

Figure 5: (a) A Typical configuration of the experimental setup. (b) Vicon motion capture system provides millimeter accuracy 6-DOF body pose tracking at 120Hz. (c) A 6-DOF freedom force plate provides single leg GRFs; (d) Control software on the robot records proprioceptive sensor measurements.

During run-time the motion capture system operates at 120Hz and records the 6-DOF robot body configuration, consisting of its cartesian position, $\mathbf{b} := [b_x, b_y, b_z] \in \mathbb{R}^3$, as well as its pitch, π, roll, ρ, and yaw γ, in the World Coordinate System, $\mathscr{W}$. Embedded force plate operates at 200 Hz and measures single leg ground reaction forces in the Plate Coordinate System, $\mathbf{F}^i_{\mathscr{P}} \in \mathscr{P}$. The subscript identifies the coordinate system where the force is represented. The superscript is the index of the leg that produced the force. The position and orientation of the Force Plate Coordinate System, $\mathscr{P}$, is measured in the beginning of every experimental session. This information is used for the computation of GRFs in the Body Coordinates, $\mathscr{B}$, as explained in Section 4.

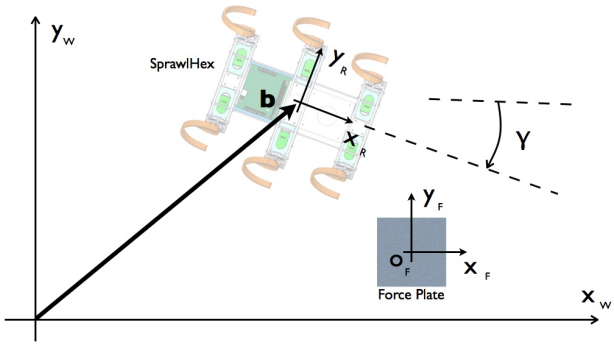

Figure 6: Various coordinate system conventions for the experimental runway. The sketch shows the horizontal plane view of the experimental setup where the robot and the force plate are shown in the World Coordinates, $\mathscr{W}$.

Figure 6 illustrates various coordinate systems and variables in relation to one another.

4 Data Collection

Authors have run two sets of experiments. The first set uses the neutral posture, $\rho = 0$, and comprises the control experiments. The second set introduces a positive sprawl posture, $\rho = 20^o$. The task-level open-loop tripod gait controller parameters [22] are kept identical in both sets of experiments. The gait for the experiments is hand tuned. The resulting gait has 50% duty cycle resulting in a very small double stance during steady state. For the preliminary stage of our work that is reported in this paper we have recorded over 1000 runs.

Each run follows a specific procedure to increase repeatability. We start the tripod gait controller as the robot is kept in the air by the experimenter. The robot is released into the runway with a positive fore/aft speed. This

manual initialization reduces the length of the transients. The first 1.5 m of the run is considered to be the transient phase and ignored in our analysis. Upon conclusion of the run the experimenter picks up the robot and presses one of its rear leg onto the force plate which serves as a common event and used for data synchronization purposes.

The raw data set consists of the body posture measurements from the motion capture system, ground reaction force measurements from the force plate, proprioceptive sensor measurements from the robot and video recordings from a camera situated on the side of the runway. These independent data streams are time synchronized using a common event that is observed by all sensory modalities.

The raw GRF measurements from the force plate are represented in the Force Plate Coordinates, $\mathscr{P}$. Typically the Body Coordinates, $\mathscr{B}$, and the Force Plate Coordinates, $\mathscr{P}$, are not aligned since the robot does not always approach the force plate along a straight line. We post process the raw GRF measurements to obtain the GRF measurements in the Body Coordinates, $\mathscr{B}$. We compute a homogenous transformation, $\mathbf{h}^{\mathscr{W}}_{\mathscr{P}} : \mathscr{P} \rightarrow \mathscr{W}$, to relate the World Coordinate System, $\mathscr{W}$, to the Plate Coordinate System, $\mathscr{P}$. Using the instantaneous body pose measurements we also construct a time-varying homogenous transformation, $\mathbf{h}^{\mathscr{B}}_{\mathscr{W}}(t) : \mathscr{W} \rightarrow \mathscr{B}$, relating the World and Body Coordinates. By a simple application of calculus we derive a time-varying transformation that allows us to compute the Body Coordinate representation of GRFs, $\mathbf{F}^{i}_{\mathscr{B}} := \mathbf{h}^{\mathscr{B}}_{\mathscr{W}} \circ \mathbf{h}^{\mathscr{W}}_{\mathscr{P}} \left(\mathbf{F}^{i}_{\mathscr{P}} \right)$.

The external video camera was used to identify which leg or legs made contact with the force plate and if the contact was clean. Those experiments where force plate contact was not proper are taken out of the GRF related analysis.

5 Experimental Results

This section presents experimental data from various experiments and their analysis. The discussions in the following subsections will compare and contrast the dynamic properties of the sprawled and neutral posture hexapods to that of arthropods.

5.1 Increased Lateral GRF

Arthropods produce significant non-propulsive lateral GRF during locomotion [28]. We hypothesized that a more sprawled posture will allow a properly tuned feed-forward driven hexapod to exert more pronounced lateral ground reaction forces during dynamical locomotion.

Our preliminary empirical data indeed confirm that there is a net increase in the total lateral ground reaction force. We observe that the change in the lateral force magnitude is most prominent in the middle leg. Figure 7 compares the average GRF for the middle leg for the neutral, $\rho = 0$, and sprawled, $\rho = 20^{o}$, posture configurations. While the fore/aft and the vertical GRFs are similar, the lateral GRF for the sprawled configuration is significantly larger that that of neutral configuration.

5.2 Differentiation of Legs

It has been shown that arthropod legs take specific roles during rapid running [1] where the front legs act like brakes, middle legs work like springs and rear legs provide propulsion. In earlier work on a neutral posture hexapod [5] this differentiation was also observed.

Averaged single leg GRF data from sprawled posture hexapod suggest that *SprawlHex* leg pairs adopt roles similar to their counterparts in arthropods. Our data suggest that the leg differentiation is stronger for the sprawled posture configuration compared to the neutral case. (Compare the black and blue average fore/aft force plots in Figure 7 Front) This is particularly interesting because the legs of *SprawlHex* are not physically differentiated, the robot is fore/aft symmetric and the controller drives all hip actuators in the same manner. Our informal observations suggest that the differentiation of the dynamic roles of legs is a direct consequence of the oscillation of the body pitch which effectively changes the load distribution during the stride.

5.3 Fore/aft Movement

In both biological systems and relevant template models the fore/aft speed is expected to decrease in the first half of a stride as the compliant legs are compressed under the momentum of the body and the kinetic energy is converted into spring potential energy. In the second half of

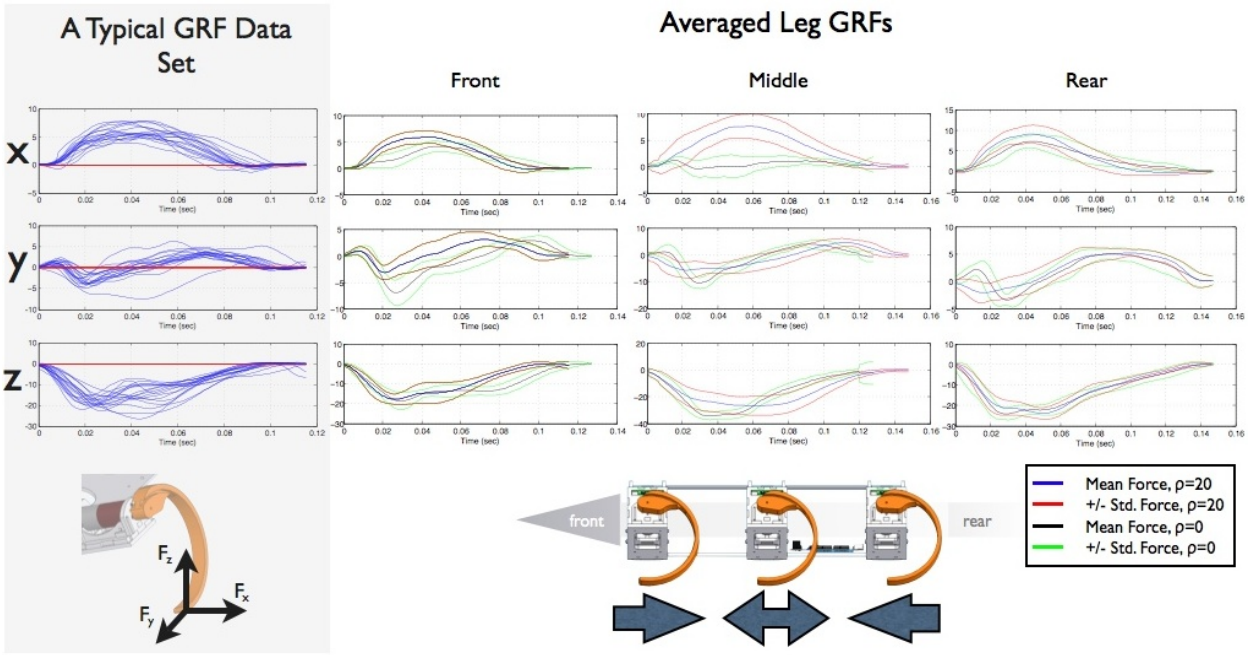

Figure 7: Single leg ground reaction force measurements. The left most column is a typical aggregate 3-DOF GRF data set for a specific leg from 100s of runs. The plots in the three columns on the right show the GRF statistics for the front, middle and rear legs. Neutral configuration, $\rho = 0$, average (black) and variance envelope (green), sprawl posture, $\rho = 20^o$, average (blue) and variance envelope (red) are shown in each plot. Forces are measured in the Body Coordinate System, $\mathscr{B}$. Notice that the fore/aft and vertical GRFs are similar whereas the magnitude of the middle leg lateral GRF is significantly larger for the sprawled posture configuration. The average of the fore/aft GRF defines a leg's dynamic role. The front leg acts as a break whose average fore/aft force is positive. The rear leg average fore/aft force is negative and indicative of a propulsive role. The middle leg fore/aft GRF averages to a small value suggesting the middle leg served as an energy storage element.

a stride this stored spring potential is returned back to the body and the COM accelerates forward.

However, our experimental data from *SprawlHex* presents a fore/aft characteristic that is different from the standard fore/aft speed pattern. Our data show that *SprawlHex* accelerates in the first half of each stride and decelerates in the second half. This fore/aft characteristic is not realizable with the standard lossless template models, such as SLIP and LLS, but it in fact requires the consideration of an actuator to provide propulsion and braking capabilities. Figure 8 illustrates the fore/aft speed and acceleration variation in relationship to the stride timing.

Physical implementation of *SprawlHex* is in fact employs active elements that inject and absorb energy from the mechanical system. Figure 9 shows that during each stride the tripod that is in ground contact does significant work on the mechanical system. This supports the earlier assertion that the observed fore/aft behavior is driven by the actions of the hip actuators. The power data in Figure 9 also suggests that there is non-zero double stance in the steady state gait which is not taken into account in standard template models and is a potential source of difference.

The data and reports from earlier studies on biological systems suggest that the steady state behavior of *SprawlHex* in fact resembles the transition gaits in animals. The

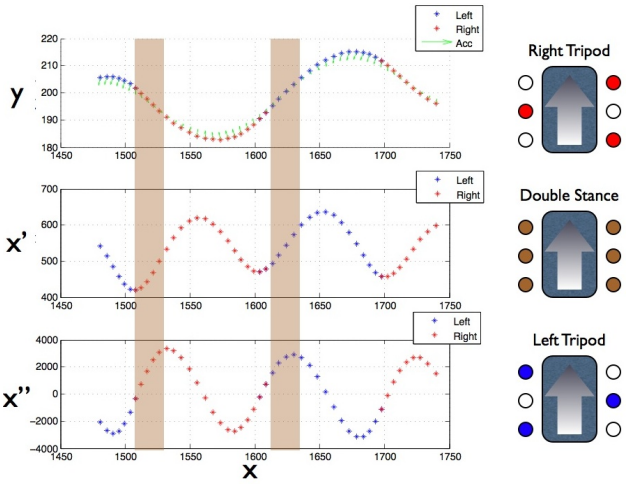

Figure 8: Horizontal plane trajectory (top) and the corresponding fore/aft speed (middle) and acceleration (bottom) of the COM. The color coding in the plots indicate which tripod is in the slow swing phase serving as a crude approximation for the ground contact period. The green arrows in the top plot are the instantaneous COM acceleration. The sketches on the right hand side illustrate the leg configurations for the right (top) and left (bottom) tripod support as well as the double stance (middle) settings. The brown time intervals are the double stance periods — when both tripods are doing work.

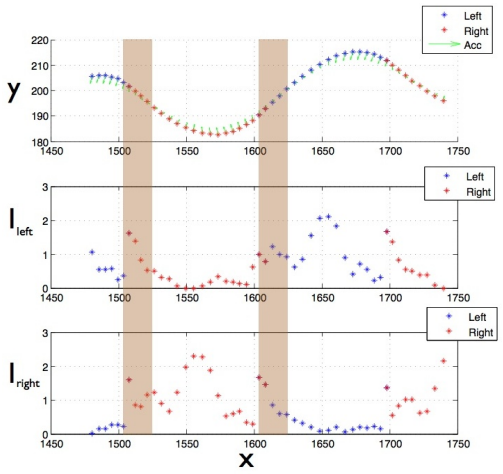

Figure 9: The COM trajectory in the horizontal plane (top) and the aggregate current consumption of the left (middle) and right (bottom) tripod actuators. The current consumption is a measure of collective work being done. The current measurement is done unsigned and does not indicate if it is positive or negative work. The brown time intervals are the double stance periods — when both tripods are doing work.

discrepancy between the *SprawlHex* and animal dynamics is the result of the incorrect tripod gait parameters [22] and that with proper tuning *SprawlHex* will demonstrate the stereotypical fore/aft acceleration pattern. In the follow up study authors will perform systematic gait optimization [30] and repeat the analysis presented in this paper.

5.4 Spatio-Temporal COM Trajectories

The neutral posture hexapod demonstrates good match in the sagittal plane dynamics but fails to capture the horizontal plane features. In contrast our data suggest that a sprawled postured hexapod platform captures the basic spatio-temporal COM trajectory patterns of not only the sagittal (SLIP) [16, 15] but also horizontal (LLS) [23, 24], plane template models.

Figure 10 presents typical steady state center of mass (COM) trajectories for neutral, $\rho = 0$, and sprawled, $\rho = 20^o$, posture hexapods as projected onto the horizontal and sagittal planes. We observe that the sagittal plane COM trajectories of the two cases are similar to one another and match the expected SLIP characteristics. On the other hand, a large difference is observed in the horizontal plane characteristics of the neutral and sprawled posture configurations. The sprawled posture configuration demonstrates large lateral swing and sizable lateral GRF. Whereas the neutral posture configuration has very small lateral GRF and an irregular and small lateral movement.

6 A Template Model

The authors identified the hip actuation and the passive compliance of the legs as two equally important players in the horizontal plane dynamics of *SprawlHex* . Fore/aft GRF of *SprawlHex* discussed in Section 5.3 cannot be

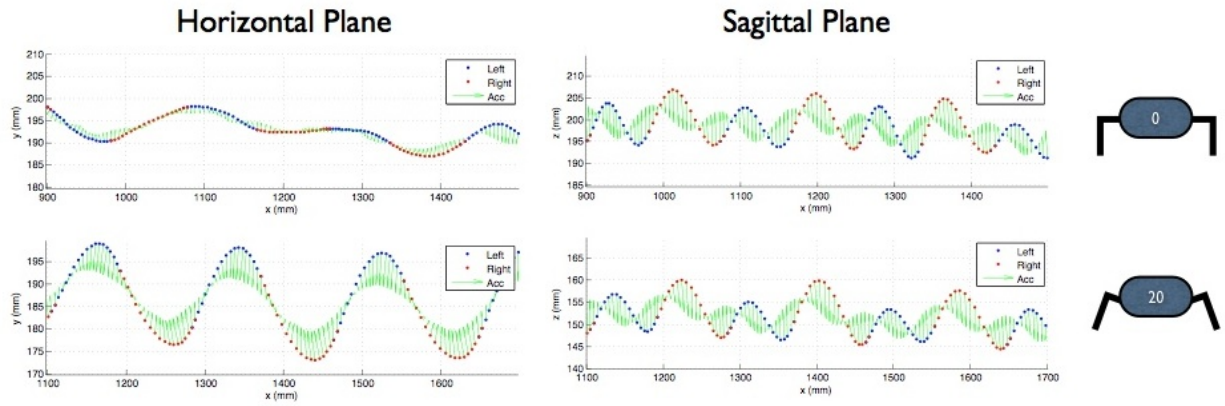

Figure 10: Representative COM trajectories for neutral (top row) and sprawl postured (bottom row) SprawlHex projected on the horizontal plane (left column) and the sagittal plane (right column). The color coding of the plots indicate which tripod is in the slow swing phase — approximately identifies the tripod supporting the body. The green arrows are the COM acceleration. The data suggest that sagittal plane dynamics of the hexapod platform does not change as a function of sprawl. Whereas the horizontal plane movement of sprawled posture configuration presents stereotypical lateral movement seen in insects.

produced by a non-actuated model. Earlier work [25] looked into actuated template models in the sagittal plane and concluded that the actuation improves the physical relevance of the simple model as well.

We posit a template model with actuation, illustrated in Figure 11. The model coasts in horizontal plane and consists of a point body mass, m, a lossless compliant prismatic leg parameterized by its rest length, l_0, and stiffness, k, and a hip actuator. The leg spring force acting on the body is

$$\mathbf{F}_s = -k\left(||\mathbf{b}-\mathbf{f}|| - l_0\right)\frac{\mathbf{b}-\mathbf{f}}{||\mathbf{b}-\mathbf{f}||}. \tag{1}$$

where $\mathbf{b}$ and $\mathbf{f}$ are the positions of the body and foot[1]. in the World Coordinate Syste, $\mathscr{W}$. An ideal torque source drives the leg about the hip joint. The hip actuator produces prescribed torque according to a time scheduled sinusoidal profile,

$$\tau = A\sin(wt+\theta). \tag{2}$$

[1]We choose to use the same variables for the horizontal plane consideration for notational simplicity

where A is the *magnitude of the actuation*, w is the *actuation frequency*, θ is the *phase of actuation*. The resulting force acting on the body due to actuation is given by

$$\mathbf{F}_a = \frac{\tau}{||\mathbf{b}-\mathbf{f}||} S \frac{\mathbf{b}-\mathbf{f}}{||\mathbf{b}-\mathbf{f}||} \quad \text{where} \quad S = \begin{bmatrix} 0 & -1 \\ 1 & 0 \end{bmatrix} \tag{3}$$

The total force acting on the body, $\mathbf{F}_t$, is the sum of the actuation force, $\mathbf{F}_a$, and the spring force, $\mathbf{F}_s$,

$$\mathbf{F}_t = \mathbf{F}_a + \mathbf{F}_s. \tag{4}$$

The template model is a hybrid dynamical system with two modes: 1) right tripod support; and 2) left tripod support. The two modes alternate without any double stance or aerial phase in between. Both right and left tripod modes are governed by the same dynamics,

$$\ddot{\mathbf{b}} = \frac{1}{m}\mathbf{F}_t. \tag{5}$$

where the foot position in the World Coordinate System, f, remains fixed. The template ignores the body yaw, γ, for simplicity. We define the leg configuration, σ, — a dependent variable — as the angle between the World's

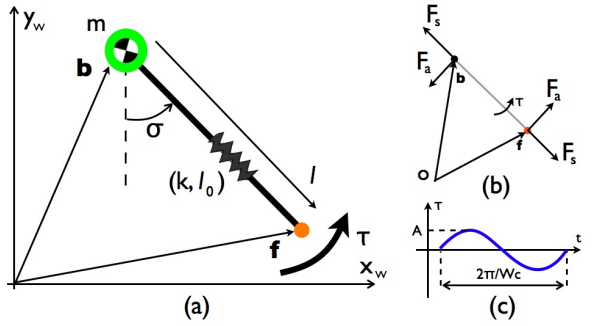

Figure 11: (a) Template model to study the horizontal plane dynamics of *SprawlHex* consists of a point mass, m riding on a lossless compliant prismatic. (b) The free body diagram of the template model. (c) The actuation model is a time schedule sinusoidal torque, τ applied to the leg. The leg is parameterized by its rest length, l_0, and stiffness, k.

lateral and the leg. Template assumes that the leg is at its rest length, $l(t = t_{TD}) = l(t = t_{LO}) = l_0$, at the touch down and lift off. The angle of attack is the leg configuration at the event of touchdown, $\sigma(t = t_T D) := \sigma_{TD}$.

7 System Identification Study

To test the viability of the proposed (preliminary) template model to characterize the behavioral characteristics of *SprawlHex* we conducted a system identification and cross validation study. For this study we setup a non-linear time-invariant regression problem where the cost function is the L2 norm of the difference between the actual COM trajectory and the trajectory produced by the model starting at the same initial condition.

$$\text{Err}^i = \left|\left| y^i_{\text{avg}} - y^i_{\text{model}} \right|\right|_{L2} \tag{6}$$

The regression problem aims to identify six parameters of the template model in Section 6: 1) leg rest length, l_0; 2) leg stiffness, k; 3) attack angle, σ_{TD}; 4) prescribed actuation magnitude, A; 5) prescribed actuation frequency, w; and 6) prescribed actuation phase offset, θ.

Run	40	28	10	19	27	29
Norm Err	1	1.09	1.20	0.96	1.15	0.93

Table 1: Normalized error in model prediction across runs. The normalized error values close to 1.0 indicate similar predictive performance as achieved on the fitting data.

Each run produces roughly 6-8 viable strides during its steady-state phase. We exclude the initial samples from each stride that correspond to double stance. Typically each stride provides roughly 10-15 viable data points which gives rise to over 60 data points for regression in each run.

Figure 12 illustrates the predictive performance of the model on two data sets: the data employed for the parameter estimation (Run #40); and the independent data set with the worst case predictive result (Run #10). To measure the performance of the template model we compute the normalized L2 difference (Equ. 7) between the average stride trajectory for a run and the model produced trajectory starting at the initial condition of the data. The Table 1 presents the results of the cross validation study for a few representative runs. The normalized error values,

$$\text{Norm Err}^i = \frac{\text{Err}^i}{\text{Err}^{40}} \tag{7}$$

are normalized with respect to the error of Run #40. The results show that the template model offers good predictive performance across all runs.

8 Conclusions

Non-propulsive lateral forces in arthropods are believed to be the source of their impressive lateral stability [11]. Recent hexapod platforms [22, 9] were specifically built to embody the sagittal plane dynamics observed in animals, which is best captured by the popular SLIP model. The *SprawlHex* with its adjustable sprawl posture design extends the focus into the horizontal plane .

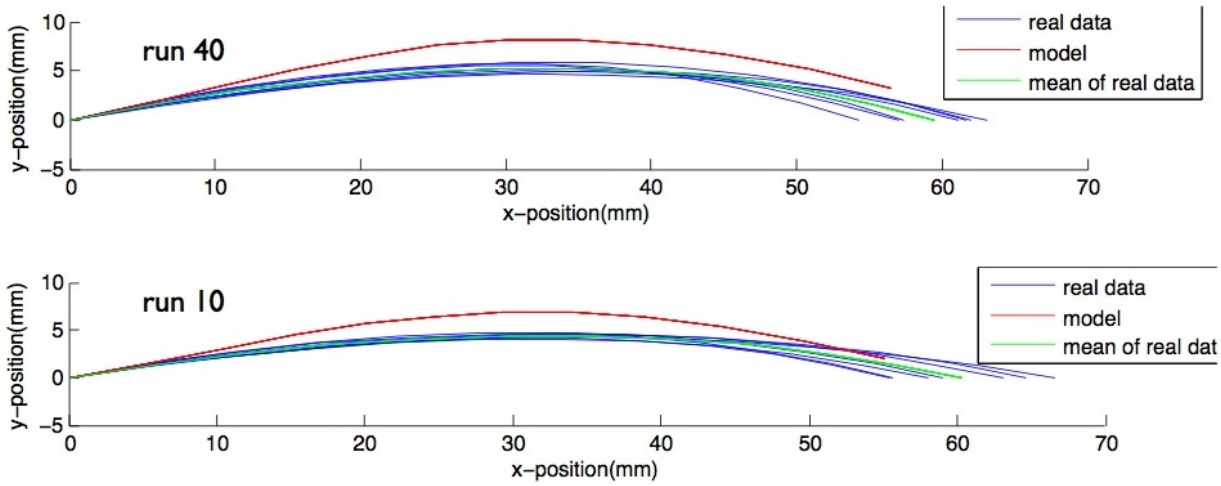

Figure 12: Cross validation of the system identification study. Each plot contains: 1) strides recorded in physical experiments (blue); 2) mean of the experimental stride trajectory (green); and 3) the trajectory produced by the fitted template model starting from the initial condition of the mean trajectory. The model parameters are identified using RUN 40. The bottom plot illustrates the performance of the model in predicting the COM trajectory.

The paper presents single leg GRF and spatio-temporal body trajectory data for the neutral, $\rho = 0$, and sprawled, $\rho > 0$, posture configurations of the robot. In comparison to the neutral postured morphology [22] the sprawled posture hexapod robot, *SprawlHex* , does produce prominent rhythmic lateral movement and larger non-propulsive lateral ground reaction forces during steady state locomotion. The dynamics of the SprawlHex does not completely match that of animals and related template models (LLS and variants). In particular, the fore/aft force of *SprawlHex* exhibits an inverse phase relationship with the lateral and vertical forces. Single leg GRFs from *SprawlHex* suggests that that the legs adopt different roles during locomotion as it was observed in biological systems.

We observe that the fore/aft acceleration of *SprawlHex* differs from that of the biological counterparts and the standard template models. *SprawlHex* heavily employs its actuators during locomotion speeding up in the first half of each stride and slowing down in the second half. The authors believe that the tripod gait parameters require further systematic optimization [30] to capture the arthropod dynamics in *SprawlHex* .

The cross validation studies suggests that a simple template model with hip actuation has consistent predictive performance across runs. The fitting study indicates that the actuation plays a strong role in shaping the ground reaction force.

In comparison to previous robotic designs [8, 22], *SprawlHex* with its horizontal and sagittal dynamic properties that have stronger resemblance to that of arthropods, is the first step towards constructing a viable physical model to study arthropod locomotion.

In dynamical systems form and function are intertwined and must be considered together in order to construct agile dynamic systems. To that end the curious effects of a simple postural configuration on the locomotion dynamics in *SprawlHex* is important to note. The role of passive mechanical properties of a locomotive platform has been shown in previous work [26]. The authors believe that a low power actuation to manipulate the body sprawl will open up a wide spectrum of new capabilities in hexapod platforms.

Our future work with *SprawlHex* will concentrate on demonstration of the use of lateral forces in highly rugged settings.

9 Acknowledgements

This work is sponsored by the NSF FIBR (EF-0425878). The authors gratefully acknowledge the contribution of Sam Russem.

References

[1] A. N. Ahn and R. J. Full. A motor and a brake: two leg extensor muscles acting at the same joint manage energy differently in a running insect. *The Journal of Experimental Biology*, 205:379–389, 2002.

[2] A. N. Ahn and Full R. J. A motor and break: Similar emgs in two adjacent leg extensor muscles result in completely different function. *American Zoologist*, 37:107A, 1997.

[3] R. Altendorfer, D. E. Koditschek, and P. Holmes. Stability analysis of a clock-driven rigid-body slip model of rhex. *International Journal of Robotics Research*, 23(10-11):1001–1012, 2004.

[4] R. Altendorfer, D. E. Koditschek, and P. Holmes. Stability analysis of legged locomotion models by symmetry-factored return maps. *International Journal of Robotics Research*, 23(10-11):979–999, 2004.

[5] R. Altendorfer, U. Saranli, H. Komsuoglu, D. E. Koditschek, Jr. H. B. Brown, M. Buehler, N. Moore, D. McMordie, and R. Full. Evidence for spring loaded inverted pendulum running in a hexapod robot. In *International Seminar on Experimental Robotics*, 2000.

[6] K. Autumn, M. Buehler, M. Cutkosky, R. J. Fearing, R. Full, D. Goldman, R. Groff, W. Provancher, A. A. Rizzi, U. Saranli, and D. E. Saunders, A. Koditschek. Robotics in scansorial environments. In *Proceedings of SPIE 2005*, pages 291–302, 2005.

[7] I.E. Brown and G.E. Loeb. A reductionist approach to creating and using neuromusculoskeletal models. In J.M. Winters and P.E. Crago, editors, *Biomechanics and Neural Control of Posture and Movement*, pages 148–191. Springer-Verlag: New York, 2000.

[8] J. G. Cham, S. A. Bailey, J. E. Clark, R. J. Full, and M. R. Cutkosky. Fast and robust: hexapedal robots via shape deposition manufacturing. *International Journal of Robotics Research*, 21(10):869–883, 2002.

[9] J. G. Cham, S. A. Beiley, and M. R. Cutkosky. Robust dynamic locomotion through feedforward-preflex interaction. In *Proceedings of ASME IMECE*, Orlando, November 5-10 2000.

[10] J. E. Clark, D. I. Goldman, P-C. Lin, G. Lynch, T. S. Chen, H. Komsuoglu, R. J. Full, and D. E. Koditschek. Design of a bio-inspired dynamical vertical climbing robot. In *Robotics Science and Systems*, 2007.

[11] M. H. Dickinson, C. T. Farley, R. J. Full, M. A. R. Koehl, R. Kram, and S. Lehman. How animals move: An integrative view. *Science*, 2000.

[12] R. J. Full, K. Autumn, J. I. Chung, and A. Ahn. Rapid negotiation of rough terrain by the death-head cockroach. *American Zoologist*, 38:81A, 1998.

[13] R. J. Full and C. T. Farley. *Musculoskeletal Dynamics in Rhythmic Systems - A Comparative Approach to Legged Locomotion*, volume Biomechanics and Neural Control of Posture and Movement, chapter Section IV: Rhythmic Systems. Springer-Verlag, New York, 2000.

[14] R. J. Full and D. E. Koditschek. Templates and anchors: Neuromechanical hypotheses of legged locomotion. *The Journal of Experimental Biology*, 202(23):3325–3332, 1999.

[15] R. M. Ghigliazza. Passively stable conservative locomotion. *SIAM Journal on Applied Dynamical Systems*, 2:187–218, 2003.

[16] R.M. Ghigliazza. A simply stabilized running model. *SIAM Review*, 47(3):519–549, 2005.

[17] D. E. Goldman, H. Komsuoglu, and D. E. Koditschek. Robots on sand. In *IEEE Spectrum*. 2008.

[18] D. I. Jindrich and R. J. Full. Dynamic stabilization of rapid hexapedal locomotion. *Journal Experimental Biology*, 205:2803–2823, 2002.

[19] H. Komsuoglu. Towards a comprehensive infrastructure for construction of modular and extensible robotic systems. Technical Report MS-CIS-07-04, Department of Computer and Information Science, University of Pennsylvania, In preparation.

[20] T. M. Kubow and R. J. Full. The role of the mechanical system in control: A hypothesis of self-stabilization in hexapedal runners. *Philosophical Transactions: Biological Sciences*, 354(1385):849–861, May 1999. Mechanisms of Neuromoscular Control (May 29, 1999).

[21] S. Revzen, M.S. Berns, Koditschek D.E., and Full R.J. Determining neuromechanical control architecture using kinematic phase response to perturbations. In *Yearly meeting of the Society for Integrative and Comparative Biology*, 2008.

[22] U. Saranli, M. Buehler, and D. E. Koditschek. Rhex - a simple and highly mobile hexapod robot. *International Journal of Robotics Research*, 20(7):616–631, 2001.

[23] J. Schmitt and P. Holmes. Mechanical models for insect locomotion: Dynamics and stability in the horizontal plane - i. theory. *Biological Cybernetics*, 83:501–515, 2000.

[24] J. Schmitt and P. Holmes. Mechanical models for insect locomotion: Dynamics and stability in the horizontal plane - ii. application. *Biological Cybernetics*, 83:517–527, 2000.

[25] J. Seipel and P. Holmes. A simple model for clock-actuated legged locomotion. *Journal of Regular and Chaotic Dynamics*, 12(5):502–520, 2007.

[26] J. C. Spagna, D. I. Goldman, P.-C. Lin, D. E. Koditschek, and R. J. Full. Distributed mechanical feedback in arthropods and robots simplifies control of rapid running on challenging terrain. *Journal of Bioinspiration and Biomimetics*, 2:9–18, 2007.

[27] A J Spence, S Revzen, K Yeates, C Mullens, and R J Full. Insects running on compliant surfaces. In *Yearly meeting of the Society for Integrative and Comparative Biology*, 2007.

[28] S. Sponberg and R. J. Full. Neuromechanical response of musculo-skeletal structures in cockroaches during rapid running on rough terrain. *Journal of Experimental Biology*, 211:433–446, 2008.

[29] J. D. Weingarten, D. E. Koditschek, H. Komsuoglu, and C. Massey. Robotics as the delivery vehicle: A contexualized, social, self paced, engineering education for life-long learners. In *Proceedings of Robotics and System Science Conference 2007*, 2007.

[30] J. D. Weingarten, G. A. D. Lopes, M. Buehler, Groff R. E., and D. E. Koditscheck. Automated gait adaptation for legged robots. In *Int. Conf. Robotics and Automation*, New Orleans, USA, 2004. IEEE.